Research Square

Preprints are preliminary reports that have not undergone peer review.
They should not be considered conclusive, used to inform clinical practice,
or referenced by the media as validated information.

Current and Future Environmental Suitability of the Nile Grass Rat (Arvicanthis niloticus) in Egypt under CMIP6 Climate Change Scenarios

Maha Mostafa

maha@sci.asu.edu.eg

Ain Shams University

Mustafa M. Soliman

Cairo University

Article

Keywords: Shared Socioeconomic Pathways, MaxEnt, Species distribution modeling, Pest management, Egypt, Zoonotic disease reservoir, Muridae, Climate change impacts

Posted Date: November 13th, 2026

DOI: https://doi.org/10.21203/rs.3.rs-10969292/v1

License: This work is licensed under a Creative Commons Attribution 4.0 International License.
Read Full License

Additional Declarations: No competing interests reported.

Abstract

The Nile grass rat (*Arvicanthis niloticus* Desmarest, 1822) is one of the most destructive agricultural rodent pests and a primary reservoir host for multiple zoonotic pathogens in Egypt, including Schistosoma mansoni, Fasciola spp., Hymenolepis nana, murine typhus, and plague (Yersinia pestis via Xenopsylla cheopis fleas). Quantifying how ongoing climate change will alter its potential geographic distribution is essential for national rodent control strategies and vector-borne disease surveillance. In this study, we calibrated an optimized Maximum Entropy (MaxEnt version 3.4.4) ecological niche model to determine the contemporary macroclimatic suitability envelope of *A. niloticus* across Egypt and projected its potential range shifts for the 2050s (2040–2060) and 2070s (2060–2080) under Phase 6 of the Coupled Model Intercomparison Project (CMIP6) Shared Socioeconomic Pathways (SSP2-4.5, moderate-emission; SSP5-8.5, high-emission). The model was calibrated using 31 spatially thinned occurrence records (rarefied with a 10 km buffer) and four non-collinear bioclimatic predictors (VIF < 5): isothermality (Bio 3), minimum temperature of the coldest month (Bio 6), mean temperature of the coldest quarter (Bio 11), and annual precipitation (Bio 12). Hyperparameter tuning using ENMeval identified Linear, Quadratic, and Hinge (LQH) feature classes with a regularization multiplier of 1.0 as the optimal configuration (lowest AICc = 646.68). Across 10-fold bootstrap cross-validation, the model demonstrated high predictive accuracy, yielding a mean training Area Under the ROC Curve (AUC) of 0.8623 ± 0.016, a mean test AUC of 0.8513 ± 0.050, and a mean True Skill Statistic (TSS) of 0.543 ± 0.142. Bio 6 emerged as the primary environmental constraint, accounting for 62.6% of the model contribution and 54.6% permutation importance, followed by Bio 11 (26.4% contribution). Using a logistic threshold of 0.245 (10th percentile training presence), approximately 570,489 km² (56.67% of Egypt) is classified within the contemporary macroclimatic suitability envelope, with high suitability concentrated across the Nile Delta, Nile Valley, Fayoum depression, and northern Mediterranean coastal plains. However, realized occupancy is strictly constrained to ~ 4%–5% of the national territory by obligate access to irrigated crops and canal water. Multi-model ensemble consensus projections reveal divergent trajectories: under SSP2-4.5, the climatically suitable envelope expands progressively to 602,952 km² (59.89%) by the 2050s and 596,981 km² (59.30%) by the 2070s under unlimited dispersal assumptions. Conversely, under the extreme SSP5-8.5 scenario, the suitable envelope contracts to 545,686 km² (54.20% of Egypt) by the 2070s—representing a 57.76% contraction of the contemporary range—driven by rising winter minimum temperatures that exceed permissive thermal baselines in Upper Egypt. Crucially, under realistic zero-dispersal constraints across hyper-arid Saharan barriers, the species experiences severe net range contraction without colonizing isolated desert regions. These findings provide vital spatial guidance for proactive rodent management and vector risk containment along current agricultural frontiers and newly reclaimed desert lands.

1. Introduction

The Nile grass rat [1] is widely recognized as the most prominent, ecologically adaptable, and economically damaging vertebrate agricultural pest in Egypt, which represents the type locality of the

species [1]. Characterized by high reproductive potential, multi-litter seasonal breeding, and opportunistic feeding, *A. niloticus* thrives along agricultural field borders, irrigation canal banks, drainage dykes, and riparian thickets [2]. In rural Egyptian agroecosystems, the species causes severe pre-harvest and post-harvest destruction to critical field crops, including faba beans (Vicia faba), wheat (Triticum aestivum), maize (Zea mays), clover (Trifolium alexandrinum), and sugarcane (Saccharum officinarum) [3]. In Upper Egypt, rodent outbreaks dominated by *A. niloticus* routinely reduce sugarcane yields by 20% to 40% and decrease sucrose extraction concentrations by up to 30%, inflicting substantial annual economic deficits on farming communities [3, 4]. Historically, annual Nile floods acted as a major natural population check by inundating burrows. However, the cessation of seasonal flooding following the construction of the Aswan High Dam, combined with permanent canal infrastructure, multi-crop perennial irrigation, and national land reclamation projects, has established permanent, stable nesting habitats that maintain chronically high rodent densities [3]. Consequently, evaluating the ecological limits and range shifts of *A. niloticus* remains a primary concern for vertebrate pest management [5, 6].

Beyond direct agricultural devastation, *Arvicanthis niloticus* is of paramount public health and veterinary concern as a primary natural reservoir host for numerous zoonotic pathogens, endoparasites, and arthropod disease vectors [7]. Because agricultural laborers, livestock, and rural dwellings exist in intimate spatial proximity to irrigated field canals, *A. niloticus* directly mediates parasite transmission cycles [7]. Parasitological surveys of wild rodents in the Nile Delta and Valley have documented high natural infection rates of zoonotic helminths in *A. niloticus*, including the dwarf tapeworm Hymenolepis nana, liver flukes (Fasciola hepatica and Fasciola gigantica), the nematode Trichosomoides nasalis [8], and the blood trematode Schistosoma mansoni, the causative agent of intestinal schistosomiasis [7].

Furthermore, *A. niloticus* serves as the primary host for ectoparasite vectors, particularly the oriental rat flea (Xenopsylla cheopis) and ixodid ticks, which transmit murine typhus (Rickettsia typhi), tick-borne borreliosis, and plague (Yersinia pestis) [9, 10]. Experimental studies have also identified *A. niloticus* as a competent reservoir host for cutaneous leishmaniasis (Leishmania major) in North Africa [11]. The continuous contact interface between rodent populations, irrigation waterways, and human settlements underscores an ongoing transmission hazard that requires systematic, spatially explicit epidemiological surveillance.

Macroclimatic regimes, particularly thermal variability and moisture availability, represent fundamental abiotic drivers of rodent demographic dynamics, reproductive timing, and broad geographic ranges [2]. In arid and semi-arid landscapes, global climate change is projected to alter temperature seasonality and extreme weather events rapidly across North Africa and the Mediterranean basin [12]. Such shifts can alter the environmental suitability of agricultural pests and disease vectors, facilitating range expansions into newly developed agricultural areas or driving local extirpations where thermal tolerances are exceeded [12, 13].

Under Phase 6 of the Coupled Model Intercomparison Project (CMIP6), Shared Socioeconomic Pathways (SSPs) provide an advanced framework to explore future distributions, contrasting intermediate-emission scenarios (SSP2-4.5) against high-emission scenarios (SSP5-8.5) [14, 15]. Ecological Niche Modeling (ENM), particularly the Maximum Entropy (MaxEnt) algorithm, has established itself as an authoritative tool for evaluating species-climate relationships from presence-only records and projecting potential distributions under future climate scenarios [16–18].

In hyper-arid countries such as Egypt, modeling species distributions presents a unique ecological duality. While macroclimate dictates the physiological thermal envelope, realized occupancy is strictly constrained by access to surface water and vegetative cover in an otherwise hyper-arid desert [19]. Although previous studies in Egypt have documented local rodent population densities, seasonal trapping indices, and parasite burdens within individual governorates, a comprehensive national-scale assessment of contemporary climatic suitability and projected future range shifts has never been conducted. To our knowledge, this study provides the first national-scale MaxEnt ecological niche model for *Arvicanthis niloticus* in Egypt under CMIP6 scenarios. Specifically, our objectives are to: (1) determine the current macroclimatic suitability envelope of *A. niloticus* across Egypt; (2) identify the key bioclimatic drivers and response thresholds governing its distribution; (3) project potential range shifts for mid-century (2050s) and late-century (2070s) under SSP2-4.5 and SSP5-8.5 using a multi-model GCM ensemble; and (4) evaluate range dynamics (expansion, contraction, stability) under contrasting dispersal assumptions. These spatial predictions provide a vital evidence base for optimizing integrated rodent pest management and targeting vector disease surveillance.

2. Materials and methods

2.1 Study area and geographic extent

The study extent encompasses the entire national territory of the Arab Republic of Egypt, situated in northeastern Africa between approximately 22°N to 32°N latitude and 24°E to 37°E longitude (Fig. 1). Egypt covers an area of approximately 1,002,450 km² and is characterized by a hyper-arid Saharan desert climate across more than 95% of its territory, receiving negligible annual precipitation (< 20 mm across central and southern regions), with modest seasonal rainfall (100–200 mm) confined to the narrow northern Mediterranean coastline. The country is divided into four primary physiographic regions: the Nile Valley and Delta, the Western (Libyan) Desert, the Eastern Desert, and the Sinai Peninsula. The fertile alluvial floodplain of the Nile River, including the Nile Delta and the Fayoum Depression, represents the primary inhabited, irrigated, and agriculturally productive corridor of the nation. In addition, isolated depression systems in the Western Desert support historic oases (Kharga, Dakhla, Farafra, Bahariya, and Siwa) sustained by fossil groundwater.

The 31 spatially thinned occurrence records of *Arvicanthis niloticus* utilized for model calibration (Fig. 1) demonstrate a pronounced, biologically consistent clustering along the Nile hydrological system. The vast majority of records are concentrated across the Nile Delta (north of ~ 29.5°N), particularly around

the delta apex and along the Damietta and Rosetta distributaries, with additional records along the northern Mediterranean coast near Alexandria. Occurrences extend southward along the linear corridor of the Nile River Valley into Upper Egypt to approximately 24°N near Lake Nasser. Importantly, the occurrence cluster situated in the Western Desert (between approximately 25.5°N and 26.5°N) corresponds directly to established agricultural cultivation and date palm plantations within the Kharga and Dakhla oasis basins of the New Valley (El-Wadi El-Gedid) governorate. These oasis records reflect localized mesic microhabitats sustained by artesian groundwater rather than natural desert environments, providing a realistic gradient of cold-season and warm-season thermal conditions across the national territory.

2.2 Species occurrence records and spatial thinning

Georeferenced occurrence records for *Arvicanthis niloticus* across Egypt were compiled from the Global Biodiversity Information Facility **(GBIF;** https://www.gbif.org/), yielding an initial dataset of 424 raw presence records. To ensure data integrity, eliminate geographic errors, and reduce spatial autocorrelation, a rigorous multi-step data cleaning protocol was executed: (1) duplicate records sharing identical coordinates were removed; (2) records lacking precise geographic coordinates or exhibiting high coordinate uncertainty (> 5 km) were discarded; (3) coordinates falling in open water bodies or outside the administrative terrestrial boundaries of Egypt were excluded; and (4) automated cleaning was performed to check for country centroids and institutional museum coordinates. To mitigate spatial sampling bias arising from dense collection effort around major research centers (Cairo, Giza, Alexandria), spatial rarefication (thinning) was performed using a 10 km Euclidean distance threshold using the spThin package in R [20]. This procedure eliminated clustered points while preserving geographic representation across the environmental gradient, resulting in a final dataset of 31 spatially independent presence records (File S1) formatted for MaxEnt modeling.

2.3 Environmental variables and multicollinearity screening

Contemporary bioclimatic variables (19 candidate predictors, Bio 1–Bio 19) representing temperature and precipitation gradients were acquired from the WorldClim database version 2.1 [21] at a spatial resolution of 2.5 arc-minutes (approximately 4.5 km at Egyptian latitudes). To avoid multicollinearity among environmental predictors that could inflate variable importance or distort model coefficients, a formal, non-circular screening procedure was conducted prior to model fitting. First, variables known to exhibit severe spatial interpolation artifacts across desert regions (Bio 8 Mean Temperature of Wettest Quarter, Bio 9 Mean Temperature of Driest Quarter, Bio 18 Precipitation of Warmest Quarter, and Bio 19 Precipitation of Coldest Quarter) were excluded beforehand. Second, precipitation variables displaying zero variance across the occurrence points (Bio 14 Precipitation of Driest Month and Bio 17 Precipitation of Driest Quarter, both representing constant 0 mm precipitation) were removed. Third, a stepwise Variance Inflation Factor (VIF) analysis was performed using the usdm package in R with a strict threshold of VIF < 5. This iterative elimination retained four final non-collinear environmental predictors: isothermality (Bio 3, VIF = 1.58), minimum temperature of the coldest month (Bio 6, VIF = 3.69), mean

temperature of the coldest quarter (Bio 11, VIF = 2.26), and annual precipitation (Bio 12, VIF = 3.08) (detailed in File S3). Although Bio 6 and Bio 11 both reflect cold-season conditions, their pairwise Pearson correlation across occurrence points was moderate (r = 0.563), allowing them to pass VIF selection and capture complementary extreme minimum vs. mean seasonal winter conditions.

All environmental layers were clipped to the national boundaries of Egypt, resampled to identical grid alignment, and converted to ASCII grid format using ArcGIS Pro [22]. Variable importance in the calibrated models was assessed through two complementary metrics: percent contribution, which measures the increase in regularized training gain attributed to each variable during model fitting, and permutation importance, which evaluates the decrease in training AUC when variable values are randomly permuted among training points [16, 17]. Jackknife evaluations of regularized training gain and test AUC were also conducted.

2.4 Future climate projections and multi-model ensemble

To project future habitat suitability for *A. niloticus*, downscaled climate projections from four General Circulation Models (GCMs) under CMIP6 were obtained from WorldClim 2.1 at a spatial resolution of 2.5 arc-minutes (~ 4.5 km): BCC-CSM2-MR, MIROC6, HadGEM3-GC31-LL, and MPI-ESM1-2-HR (File S4). These GCMs were selected for their proven reliability and widespread application in North African and Mediterranean ecological impact assessments [23–26]. Future climate surfaces were evaluated for two time horizons: the 2050s (average for 2040–2060) and the 2070s (average for 2060–2080). For each time slice, two contrasting Shared Socioeconomic Pathways were evaluated: SSP2-4.5 (the intermediate-emission / moderate-emission 'middle-of-the-road' pathway, assuming balanced socioeconomic development and radiative forcing stabilizing at 4.5 W/m² by 2100) and SSP5-8.5 (the high-emission 'fossil-fueled development' pathway, representing an upper-bound forcing of 8.5 W/m² by 2100) [14, 15].

All future raster layers were clipped to the Egyptian territory and converted to ASCII format in ArcGIS Pro. When projecting models to future scenarios, MaxEnt clamping was enabled to constrain extreme values and prevent unrealistic mathematical extrapolations in novel environmental spaces. To account for structural uncertainties inherent in individual climate models, a multi-model ensemble consensus approach was implemented. The calibrated MaxEnt model was projected onto each GCM surface independently, and the resulting continuous cloglog suitability maps were averaged pixel-by-pixel for each SSP and time-period combination, producing consensus future suitability models.

2.5 Model evaluation, hyperparameter tuning, and threshold selection

Species distribution modeling was performed using MaxEnt version 3.4.4 [18]. MaxEnt estimates the target probability distribution by finding the probability distribution of maximum entropy subject to constraints defined by observed occurrence data and environmental background points [17]. To prevent model overfitting and minimize complexity, a critical step when working with small sample sizes model hyperparameters were systematically optimized using the ENMeval package in R [27]. Candidate models

were constructed by evaluating combinations of feature classes (Linear [L], Quadratic [Q], Hinge [H], Product [P]) across regularization multipliers (RM) from 0.5 to 4.0 in increments of 0.5. Model performance was evaluated using the corrected Akaike Information Criterion (AICc), which penalizes parameter over-complexity [28]. The optimal configuration was the model utilizing Linear, Quadratic, and Hinge (LQH) features with RM = 1.0, achieving the lowest AICc value of 646.68 (File S5).

Model validation was conducted using a bootstrap resampling procedure with 10 replicates. In each iteration, 70% of the occurrence records (n = 22) were randomly assigned for model training, and the remaining 30% (n = 9) were set aside for independent testing against 10,000 background points sampled across Egypt. Predictive accuracy was assessed using the Area Under the Receiver Operating Characteristic Curve (AUC) and the True Skill Statistic (TSS). AUC values above 0.8 indicate good discriminatory performance, while TSS values above 0.5 indicate good classification accuracy [29, 30]. To convert continuous MaxEnt cloglog suitability values (0–1) into binary presence-absence distributions for spatial area calculations and range shift dynamics, a logistic threshold of 0.245 (corresponding to the 10th percentile training presence / equate entropy threshold) was applied. This threshold minimizes commission errors across barren desert environments while ensuring complete sensitivity across confirmed agricultural populations. Habitat range dynamics were categorized into four classes: stable presence, range expansion, range contraction, and stable absence. Finally, to evaluate the influence of dispersal constraints across hyper-arid barriers, we evaluated two scenarios: (1) unlimited dispersal (species occupies all climatically suitable pixels), and (2) zero dispersal (future range is restricted to currently occupied pixels that remain suitable).

3. Results

3.1 Model performance and key environmental drivers

The calibrated MaxEnt model for *Arvicanthis niloticus* demonstrated robust predictive accuracy and high consistency across bootstrap replicates. The mean training AUC was 0.8623 ± 0.016, and the mean test AUC was 0.8513 ± 0.050 (Fig. 2, File S6). Model classification performance was further corroborated by the True Skill Statistic (TSS), which yielded a mean value of 0.543 ± 0.142 under the 0.245 threshold, demonstrating significant discriminatory capacity to distinguish suitable environmental envelopes from hyper-arid background environments.

Analysis of variable importance identified the minimum temperature of the coldest month (Bio 6) as the dominant environmental driver governing *A. niloticus* distribution in Egypt, accounting for 62.6% of the model's percent contribution and 54.6% of permutation importance (Table 1). The mean temperature of the coldest quarter (Bio 11) was the second most influential predictor, with a percent contribution of 26.4% and a permutation importance of 31.4%. Together, these two cold-season thermal metrics accounted for 89.0% of the model's overall contribution. Annual precipitation (Bio 12) contributed 7.7% (permutation importance 8.9%), while isothermality (Bio 3) accounted for 3.4% (permutation importance 5.1%). The Jackknife evaluation (File S7) corroborated these findings: Bio 6 provided the highest

regularized training gain and test AUC when modeled in isolation, confirming it as the single most informative predictor. Conversely, omitting Bio 11 produced the largest decrease in regularized gain, indicating that it contains the greatest amount of unique predictive information not captured by the other variables.

Table 1
Percent contributions and permutation importance of environmental predictors in the calibrated MaxEnt model for *Arvicanthis niloticus* based on ten bootstrap replicates.

Variable	Description	Percent Contribution (%)	Permutation Importance (%)
Bio 6	Minimum temperature of the coldest month	62.6	54.6
Bio 11	Mean temperature of the coldest quarter	26.4	31.4
Bio 12	Annual precipitation	7.7	8.9
Bio 3	Isothermality [BIO2/BIO7] (× 100)	3.4	5.1

Percent contributions sum to 100.1% due to individual rounding of percentages. Permutation importance values reflect the decline in AUC when variable values are randomly permuted among presence and background points.

3.2 Climatic niche preferences and response curves

Marginal and isolated response curves illustrate clear thermal and hydrological thresholds for *A. niloticus* in Egypt (File S8). For the minimum temperature of the coldest month (Bio 6), the isolated response curve displays a distinct unimodal peak at approximately 7.22°C, with suitability declining sharply at temperatures below 5°C and above 10°C. In the full marginal model, suitability remains high across a broader range, peaking at 16.4°C before declining. The response curve for the mean temperature of the coldest quarter (Bio 11) exhibits an optimal suitability window between 14.1°C and 14.3°C, with steep declines below 12°C and above 18°C, highlighting high sensitivity to winter cold-season thermal boundaries.

For annual precipitation (Bio 12) in isolation, predicted suitability rises progressively with increasing rainfall, starting from 0.64 at 0 mm and reaching optimal suitability (~ 0.97) near 203.5 mm. Crucially, however, in the full marginal model, suitability remains persistently high (> 0.79) across the entire precipitation gradient from 0 to 250 mm. This indicates that under Egyptian conditions, local rainfall is not a strictly limiting factor because the species is ecologically buffered by access to perennial riverine and canal irrigation. Finally, suitability for isothermality (Bio 3) peaks at 33.0% when modeled in isolation, and at 53.1% in the marginal model.

3.3 Current habitat suitability and geographical distribution

Under contemporary climatic conditions, the model predicts that approximately 570,489 km² of Egypt's land surface falls within the climatically suitable envelope (suitability > = 0.245), representing 56.67% of the national territory (Fig. 3). Areas of high suitability (deep crimson) are strongly clustered within the Nile Delta, the Cairo–Giza metropolitan region, the Fayoum Depression, and along the linear fertile corridor of the Nile River Valley extending south toward Aswan. High suitability is also mapped along the northern Mediterranean coastal strip from Salloum in the west to Rafah in the east. Scattered patches of moderate suitability are identified in the coastal plains of Matrouh, the cultivated oasis systems of the New Valley (Kharga, Dakhla, Farafra), and isolated foothills in Sinai and along the Red Sea coast. However, as evaluated below, realized occupancy in Egypt is strictly confined to ~ 4%–5% of the land area where irrigation infrastructure supports crops and damp soils.

3.4 Future range dynamics and shift scenarios

Multi-model ensemble consensus projections project substantial redistributions of suitable habitat for *A. niloticus* across Egypt under both SSP2-4.5 and SSP5-8.5 for the 2050s and 2070s (Figs. 4 and 5; Table 2). Under the moderate-emission scenario (SSP2-4.5) by the 2050s, the climatically suitable area increases to 602,952 km² (59.89% of Egypt), representing a net gain of 32,463 km² (+ 5.69% relative to current conditions). This net change reflects a 41.12% expansion into newly suitable regions offset by a 35.43% contraction of currently suitable areas. By the 2070s under SSP2-4.5, the suitable area stabilizes at 596,981 km² (59.30% of Egypt), comprising an expansion of 52.99% and a contraction of 48.34%, yielding a net gain of 26,492 km² (+ 4.64%) under unlimited dispersal.

Under the high-emission scenario (SSP5-8.5), habitat dynamics exhibit pronounced volatility. In the 2050s, the suitable area increases modestly to 583,197 km² (57.93% of Egypt; net gain of + 12,708 km² or + 2.23%), driven by an expansion of 46.51% and a contraction of 44.28%. By the 2070s, however, the potential distribution undergoes a net contraction to 545,686 km² (54.20% of Egypt), representing a net loss of 24,803 km² (-4.35% relative to contemporary range). This late-century decline is driven by an extensive 57.76% contraction of currently occupied territory, which outweighs the 53.41% expansion into previously unsuitable regions.

Table 2
Predicted current and future suitable habitat area (km² and %) for *Arvicanthis niloticus* under SSP2-4.5 and SSP5-8.5 climate change scenarios for 2050 and 2070 based on the 0.245 logistic threshold.

Period	Scenario	Current Area (km²)	Current Area (%)	Future Area (km²)	Future Area (%)	Expansion (%)	Contraction (%)
2050	SSP2-4.5	570,489	56.67	602,952	59.89	41.12	35.43
2050	SSP5-8.5	570,489	56.67	583,197	57.93	46.51	44.28
2070	SSP2-4.5	570,489	56.67	596,981	59.30	52.99	48.34
2070	SSP5-8.5	570,489	56.67	545,686	54.20	53.41	57.76

Current Area (%) and Future Area (%) are expressed as percentages of the total terrestrial study area of Egypt (1,002,450 km²). Expansion (%) and Contraction (%) are expressed relative to the contemporary suitable habitat area (570,489 km²). Under an unlimited dispersal assumption, net area equals Future Area. Under a zero-dispersal assumption across hyper-arid barriers, expansion is zero and net change is governed strictly by range contraction (-35.43% to -57.76%).

Spatial analysis of the binary change maps (Fig. 5) reveals consistent geographical patterns across all four scenarios. Stable presence (green) is preserved across the core breadbaskets of the Nile Delta, the Fayoum Depression, and the northern Nile Valley. Range expansion (blue) is projected primarily across the central Sinai plateau, the northwestern Mediterranean hinterlands, and localized depression corridors in the Western Desert. Conversely, range contraction (red) is heavily concentrated along the southern limits of the Nile Valley in Upper Egypt (Aswan, Luxor, Qena), the Red Sea coastal foothills, and southern Sinai. In Upper Egypt, projected warming under SSP5-8.5 raises winter minimum temperatures beyond the optimal thermal envelope, causing a progressive northward retreat of suitable climatic space.

Crucially, comparing dispersal assumptions fundamentally alters the biological interpretation of these projections. Under an unlimited dispersal assumption, the species achieves modest net expansions (+ 2.2% to + 5.7%) across three scenarios. However, because *A. niloticus* cannot naturally cross 100–300 km of open Saharan sand dunes to reach isolated 'newly suitable' desert patches, an ecologically realistic zero-dispersal scenario reveals that the species will not realize this desert expansion. Instead, it will suffer a direct net range contraction of 35.43% to 48.34% under SSP2-4.5, and up to 57.76% under SSP5-8.5, indicating severe climate-induced range degradation across its southern range.

4. Discussion

Anthropogenic climate change is profoundly restructuring the geographic ranges, phenological schedules, and population outbreaks of agricultural pests and zoonotic disease vectors worldwide,

posing formidable challenges to food security and public health in hyper-arid regions [12, 31]. For rodent pests, which are characterized by rapid reproduction, broad dietary adaptability, and high sensitivity to microclimatic fluctuations, shifts in seasonal temperature and rainfall can trigger dramatic demographic booms and spatial realignments (Sicard et al., 2004a, 2004b). In this study, we developed the first national-scale ecological niche model for *Arvicanthis niloticus* in Egypt under CMIP6 climate scenarios, establishing an objective baseline to assess current exposure and anticipate future redistribution across national agroecosystems.

Long-term demographic and ecological field studies in West Africa (Burkina Faso and Mali) have established that breeding activity, litter frequency, and population explosions of *A. niloticus* are intimately tied to rainfall seasonality, minimum temperatures, relative humidity, and primary food productivity [2]. Despite this sensitivity, explicit ecological niche models evaluating the contemporary and future climatic distribution of *A. niloticus* have remained scarce across North Africa. Our application of MaxEnt with ENMeval hyperparameter tuning provided robust discriminatory accuracy (test AUC = 0.851, TSS = 0.543) while penalizing over-parameterization, confirming that MaxEnt is uniquely well-suited for presence-only data with small sample sizes when tuned objectively [27, 32].

A critical conceptual finding of this study is the marked disparity between the modeled macroclimatic suitability envelope (~ 570,489 km², or 56.67% of Egypt) and the species' realized geographic distribution. In reality, *A. niloticus* is strictly confined to approximately 4%–5% of the Egyptian land surface—predominantly the alluvial plain of the Nile Delta, the narrow ribbon of the Nile River Valley, the Fayoum Depression, and cultivated oases. This divergence is readily explained by the BAM framework. The MaxEnt model maps the abiotic macroclimatic envelope (A), identifying regions where temperature seasonality and macro-scale humidity are theoretically permissive. However, because *A. niloticus* is an obligate mesic herbivore with high water turnover rates, its survival depends strictly on biotic factors (B; dense herbaceous canopies, grain crops, weed cover) and local hydrological factors (permanent canal water, moist burrowing soils) that are completely absent from the open Saharan desert. This disconnect is demonstrated by the response curve for annual precipitation (Bio 12), where predicted suitability remains uniformly high (> 0.79) across all rainfall levels (0 to 250 mm). In Egypt, the perennial Nile hydrological network and extensive canal infrastructure decouple rodent survival from local rainfall, creating an artificial microhabitat that buffers arid macroclimatic extremes [19]. Consequently, while vast tracts of the Western Desert and Sinai fall within the permissive macroclimatic envelope, they remain completely uninhabited due to the absence of surface water and vegetative cover. However, this macroclimatic permeability poses an active invasion risk: as Egypt expands mega-irrigation reclamation projects into desert plateaus (e.g., the Toshka Project, the New Valley Scheme, and the New Delta megaproject), artificial canal extensions inadvertently provide the missing biotic and hydrological requisites, transforming formerly barren desert into highly suitable rodent habitats.

Among the environmental predictors, the minimum temperature of the coldest month (Bio 6) and the mean temperature of the coldest quarter (Bio 11) exerted overwhelming dominance, collectively accounting for 89.0% of the model contribution and 86.0% of permutation importance. This strong

dependency aligns closely with murid physiological ecology. In arid and semi-arid environments, winter minimum temperatures govern metabolic energy expenditure, burrow emergence schedules, and the termination of reproductive diapause [33, 34]. Milder winter minimums (Bio 6 ~ 7°C to 16°C) reduce cold-induced thermoregulatory stress, extend nocturnal foraging activity, and permit earlier reproductive onset, driving rapid population growth [2]. Conversely, extreme cold suppresses above-ground activity. Interestingly, while our model excluded summer extreme heat variables (Bio 5 and Bio 10) due to multicollinearity screening, the steep decline in suitability observed in isolated Bio 6 (> 10°C) and Bio 11 (> 18°C) curves suggests that *A. niloticus* is adapted to contemporary winter baselines. When future winter minimum temperatures exceed these historical thresholds, as projected under SSP5-8.5 in Upper Egypt, the physiological and phenological synchronization of the species is disrupted, driving projected southern habitat contractions.

Consensus projections across CMIP6 scenarios demonstrate that future range shifts will be governed by the intensity of greenhouse gas emissions. Under moderate warming (SSP2-4.5), the climatically suitable envelope expands by 4.6% to 5.7% through the 2050s and 2070s, as warmer winter nights make cooler northern desert plateaus and elevated Sinai terrains climatically accessible. Under the extreme emission pathway (SSP5-8.5), however, a net range contraction (-4.35%) occurs by 2070, characterized by a massive 57.76% contraction of currently suitable habitats. This contraction is heavily concentrated in Upper Egypt (Luxor, Aswan, Lake Nasser corridor), where projected warming exceeds the species' optimal cold-season baseline. More importantly, when evaluated through the lens of dispersal barriers, the reality of these range shifts becomes stark. Because *A. niloticus* is a terrestrial murid with typical dispersal distances < 1 km along vegetated ditches, it is physically incapable of naturally traversing hundreds of kilometers of hyper-arid gravel and sand seas to reach 'newly suitable' patches in central Sinai or the Western Desert. Under an ecologically realistic zero-dispersal scenario, future expansion into desert regions is zero, and the species will experience an unmitigated net range contraction of 35.43% to 57.76% across its contemporary range. Realized expansion will only occur if humans inadvertently transport rodents via agricultural supply trucks or construct continuous agricultural canal corridors.

These spatial dynamics provide valuable biogeographical comparisons with other African murids. In South Africa, ecological niche models for commensal Rattus species (Rattus rattus, R. norvegicus, and R. tanezumi) indicated that their potential distributions were predominantly governed by temperature seasonality, precipitation, and urban infrastructure, which buffer environmental extremes [35]. While Rattus species are closely linked to urban buildings and refuse, *A. niloticus* exhibits a specialized niche tied to rural agroecosystems, open agricultural fields, and canal dykes [36]. Thus, whereas commensal rats rely on urban infrastructure to overcome climatic limitations, *A. niloticus* relies on agricultural irrigation infrastructure, making its spatial distribution uniquely susceptible to shifts in agricultural water availability and cropping patterns.

Our macroclimatic findings are strongly corroborated by empirical seasonal trapping surveys from Upper Egypt. In Sohag Governorate, multi-year surveys have revealed notable temporal shifts in *A. niloticus*

abundance. During 2012–2013, Desoky et al. (2014)[37] reported that *A. niloticus* was trapped predominantly in winter, followed by summer and autumn, reflecting a winter-adapted activity peak. However, subsequent surveys in newly cultivated reclaimed areas (El-Kawther, 2014–2016) demonstrated a shift toward autumn and summer dominance, with lowest abundance in winter [3]. More recently, surveys in Abydos (2021–2022) confirmed an autumn-summer dominance across agroecosystems [38]. This progressive seasonal shift toward warmer post-harvest periods in Upper Egypt suggests that *A. niloticus* is actively adjusting its phenology in response to warmer winter baselines and altered crop harvesting schedules, providing empirical support for our model's inference that winter thermal regimes and water availability jointly dictate population viability.

While this study provides the first national assessment of *A. niloticus* under CMIP6 scenarios, several methodological limitations must be acknowledged. First, presence-only models are susceptible to spatial collection bias, although this was mitigated through 10 km spatial thinning. Second, validating models with 31 thinned occurrences yields relatively small test partitions (n = 9), although performance was stabilized via ENMeval hyperparameter tuning and 10-fold bootstrap averaging. Third, macroclimatic predictors cannot capture fine-scale microclimates within rodent burrows or crop canopies. Future research should integrate high-resolution remote sensing layers (e.g., NDVI, land-use/land-cover, soil moisture, and distance to irrigation canals) and demographic trapping data to model the realized agricultural niche directly. Nevertheless, the current macroclimatic models provide an indispensable foundation for anticipating broad-scale range dynamics and guiding risk-based rodent control and zoonotic disease surveillance in a warming Egypt.

5. Conclusion

This study provides the first national-scale ecological niche model evaluating the contemporary and future environmental suitability of the Nile grass rat (*Arvicanthis niloticus*) across Egypt under CMIP6 climate change scenarios. Our results demonstrate that cold-season temperatures, particularly the minimum temperature of the coldest month (Bio 6) and mean temperature of the coldest quarter (Bio 11), are the primary macroclimatic drivers governing its potential distribution. While more than half of Egypt falls within the permissive macroclimatic suitability envelope (56.67%), realized occupancy is strictly confined to ~ 4%–5% of the land area where perennial Nile irrigation networks sustain crops and vegetative cover. Future projections reveal divergent range dynamics: under moderate warming (SSP2-4.5), the suitable envelope expands modestly through the 2070s, whereas extreme warming (SSP5-8.5) triggers a net contraction by 2070, characterized by a 57.76% contraction of currently suitable range in Upper Egypt as winter minimums depart from historical baselines. When realistic zero-dispersal constraints are considered across hyper-arid Saharan barriers, expansion into isolated desert plateaus is non-viable, resulting in severe net range contraction for resident populations. These spatial insights provide critical decision-support for agricultural authorities and public health agencies, demonstrating the urgent need to integrate targeted rodent management and vector surveillance into national land reclamation programs and irrigation expansions across Egypt.

Declarations

Funding

The authors declare that no funds, grants, or other support were received during the preparation of this manuscript.

Declaration of Generative AI and AI-assisted technologies in the writing process

The authors utilized artificial intelligence tools solely for grammatical correction and linguistic refinement to ensure the clarity of the manuscript. The final version was thoroughly reviewed and approved by the authors.

Competing Interests

The authors have no relevant financial or non-financial interests to disclose.

Data availability

All data generated or analysed during this study are included in this published article and its supplementary information files.

Author Contribution

M.M did the practical analysis, prepared tables, and wrote the first draft of the article. S.M prepared the figures and wrote, edited and revised the article. All authors reviewed the manuscript.

References

1. Desmarest, A.-G., & Bénard, R. (1820). Mammalogie, ou, Description des espèces de mammifères. Chez Mme. Veuve Agasse, imprimeur-libraire. https://doi.org/10.5962/bhl.title.59887.
2. Sicard, B., Maurel, D., Fuminier, F., & Boissin, J. (1994). Climate, trophic factors, and breeding patterns of the Nile grass rat (Arvicanthis niloticus solatus): A 5-year study in the Sahelian region of Burkina Faso (formerly Upper Volta). Canadian Journal of Zoology, 72(2), 201–214. https://doi.org/10.1139/z94-027.
3. Ss Desoky, A. E.-A. (2019). Survey and Seasonal Distribution of the Rodents in El- Kawther City, Sohag Governorate, Egypt. World Journal of Agriculture and Soil Science, 2(1). https://doi.org/10.33552/WJASS.2019.02.000527.
4. El-Shafie, H. A. F., & Abdel-Banat, B. M. A. (2018). Non-arthropod pests of date palm and their management. CABI Reviews, 1–13. https://doi.org/10.1079/PAVSNNR201813020.
5. Ashry, M., Hassan, Z., Wilson, M., Moustafa, M., & Taha, A. (2024). Evaluating the Anti-fertility Potentials of 3-Monochloropropane-1, 2-diol (Alpha-Chlorohydrin) and Testosterone in Adult Male

Wild Nile Grass Rats (Arvicanthis niloticus) for Rodent Control. Iranian Journal of Toxicology, 18(1), 29–38. https://doi.org/10.61186/IJT.18.1.29.

6. Omar, S., El-Tantawi, H., Soliman, S., & Taha, A. (2023). Evaluating the effects of quinestrol on the reproductive organs of the Nile rat (Arvicanthis niloticus) for use in the rat control. Egyptian Journal of Basic and Applied Sciences, 10(1), 875–893. https://doi.org/10.1080/2314808X.2023.2290837.
7. Youssef, A. I., & Uga, S. (2014). Review of Parasitic Zoonoses in Egypt. Tropical Medicine and Health, 42(1), 3–14. https://doi.org/10.2149/tmh.2013-23.
8. Diagne, M., Vuong, P. N., Duplantier, J. M., Ba, K., Thirion-Lochouarn, L., Attout, T., & Bain, O. (2004). Histological study of Trichosomoides nasalis (Nematoda: Trichinelloidea) in the nasal cavities of the murid Arvicanthis niloticus, with associated pathology. Parasite, 11(4), 351–358. https://doi.org/10.1051/parasite/2004114351.
9. S. Farid, D., M. Abouelhassan, E., A. El- Sebae, A., E. Enany, M., & I. Youssef, A. (2020). Ectoparasite Fauna of Commensal Rodents Collected from the North Sinai Governorate—Egypt and its Public Health Significance. Advances in Animal and Veterinary Sciences, 9(4). https://doi.org/10.17582/journal.aavs/2021/9.4.563.570.
10. Panagiotakopulu, E. (2004). Pharaonic Egypt and the origins of plague. Journal of Biogeography, 31(2), 269–275. https://doi.org/10.1046/j.0305-0270.2003.01009.x.
11. Sadlova, J., Vojtkova, B., Hrncirova, K., Lestinova, T., Spitzova, T., Becvar, T., Votypka, J., Bates, P., & Volf, P. (2019). Host competence of African rodents Arvicanthis neumanni, A. niloticus and Mastomys natalensis for Leishmania major. International Journal for Parasitology: Parasites and Wildlife, 8, 118–126. https://doi.org/10.1016/j.ijppaw.2019.01.004.
12. El-Hawagry, M. S. A., Al-Akeel, R., Almadiy, A., Al Dhafer, H. M., & Soliman, M. M. (2026). Climate-driven distribution modeling of Glossina fuscipes (Diptera: Glossinidae) in the Afrotropical Region: current patterns, future projections, and implications for presence in the Arabian Peninsula. Environmental Monitoring and Assessment, 198(5), 558. https://doi.org/10.1007/s10661-026-15355-5.
13. Soliman, M. M., El-Hawagry, M. S. A., & Samy, A. M. (2025). Re-emergence of Aedes aegypti (Linnaeus) in Egypt: Predicting distribution shifts under climate changes. Medical and Veterinary Entomology, 39(3), 548–558. https://doi.org/10.1111/mve.12794.
14. O'Neill, B. C., Kriegler, E., Ebi, K. L., Kemp-Benedict, E., Riahi, K., Rothman, D. S., Van Ruijven, B. J., Van Vuuren, D. P., Birkmann, J., Kok, K., Levy, M., & Solecki, W. (2017). The roads ahead: Narratives for shared socioeconomic pathways describing world futures in the 21st century. Global Environmental Change, 42, 169–180. https://doi.org/10.1016/j.gloenvcha.2015.01.004.
15. Riahi, K., Van Vuuren, D. P., Kriegler, E., Edmonds, J., O'Neill, B. C., Fujimori, S., Bauer, N., Calvin, K., Dellink, R., Fricko, O., Lutz, W., Popp, A., Cuaresma, J. C., Kc, S., Leimbach, M., Jiang, L., Kram, T., Rao, S., Emmerling, J., … Tavoni, M. (2017). The Shared Socioeconomic Pathways and their energy, land use, and greenhouse gas emissions implications: An overview. Global Environmental Change, 42, 153–168. https://doi.org/10.1016/j.gloenvcha.2016.05.009.

16. Elith, J., Phillips, S. J., Hastie, T., Dudík, M., Chee, Y. E., & Yates, C. J. (2011). A statistical explanation of MaxEnt for ecologists: Statistical explanation of MaxEnt. Diversity and Distributions, 17(1), 43–57. https://doi.org/10.1111/j.1472-4642.2010.00725.x.
17. Phillips, S. J., Anderson, R. P., & Schapire, R. E. (2006). Maximum entropy modeling of species geographic distributions. Ecological Modelling, 190(3–4), 231–259. https://doi.org/10.1016/j.ecolmodel.2005.03.026.
18. Phillips, Steven J.; Dudík, Miroslav; Schapire, Robert E. (2024). Maxentsoftwareformodelingspeciesnichesanddistributions (Version 3.4.4) [Computer software]. https://biodiversityinformatics.amnh.org/open_source/maxent/?utm_source=chatgpt.com.
19. Fouad, S. S., Heggy, E., Ramah, M., Abotalib, A. Z., Palmer, E. M., Jomaa, S., & Weilacher, U. (2023). Egypt's waterways conservation campaigns under growing intrinsic demand and Nile upstream damming. Journal of Hydrology: Regional Studies, 50, 101537. https://doi.org/10.1016/j.ejrh.2023.101537.
20. Hosni, E. M., Nasser, M. G., Al-Ashaal, S. A., Rady, M. H., & Kenawy, M. A. (2020). Modeling current and future global distribution of Chrysomya bezziana under changing climate. Scientific Reports, 10(1), 4947. https://doi.org/10.1038/s41598-020-61962-8.
21. Fick, S. E., & Hijmans, R. J. (2017). WorldClim 2: New 1-km spatial resolution climate surfaces for global land areas. International Journal of Climatology, 37(12), 4302–4315. https://doi.org/10.1002/joc.5086.
22. Environmental Systems Research Institute (ESRI). (2020). ArcGISPro (Version 2.8) [Computer software]. Environmental Systems Research Institute (ESRI). https://pro.arcgis.com/en/pro-app/2.8/get-started/arcgis-pro-system-requirements.htm.
23. Harris, R. M. B., Grose, M. R., Lee, G., Bindoff, N. L., Porfirio, L. L., & Fox-Hughes, P. (2014). Climate projections for ecologists. WIREs Climate Change, 5(5), 621–637. https://doi.org/10.1002/wcc.291.
24. Islam, Md. T., Shalehin, M., Jahan, N., Islam, Md. R., Akash, & Adham, A. K. M. (2024). Modeling Boro rice water requirements and irrigation schedules in Mymensingh, Bangladesh, under subtropical climate change. Results in Engineering, 24, 103665. https://doi.org/10.1016/j.rineng.2024.103665.
25. Tran, T.-N.-D., & Lakshmi, V. (2024). Enhancing human resilience against climate change: Assessment of hydroclimatic extremes and sea level rise impacts on the Eastern Shore of Virginia, United States. Science of The Total Environment, 947, 174289. https://doi.org/10.1016/j.scitotenv.2024.174289.
26. Zhang, P., Zhou, P., Liu, Y., Xu, Z., Gong, L., & Xiang, X. (2025). Distribution Dynamics of Wide-Ranged and Narrow-Ranged Species From the Pliocene to the Future: Insights From Asian Endemic Holcoglossum (Orchidaceae). Ecology and Evolution, 15(4), e71301. https://doi.org/10.1002/ece3.71301.
27. Morales, N. S., Fernández, I. C., & Baca-González, V. (2017). MaxEnt's parameter configuration and small samples: Are we paying attention to recommendations? A systematic review. PeerJ, 5, e3093. https://doi.org/10.7717/peerj.3093.

28. Warren, D. L., & Seifert, S. N. (2011). Ecological niche modeling in Maxent: The importance of model complexity and the performance of model selection criteria. Ecological Applications, 21(2), 335–342. https://doi.org/10.1890/10-1171.1.
29. Allouche, O., Tsoar, A., & Kadmon, R. (2006). Assessing the accuracy of species distribution models: Prevalence, kappa and the true skill statistic (TSS). Journal of Applied Ecology, 43(6), 1223–1232. https://doi.org/10.1111/j.1365-2664.2006.01214.x.
30. Swets, J. A. (1988). Measuring the Accuracy of Diagnostic Systems. Science, 240(4857), 1285–1293. https://doi.org/10.1126/science.3287615.
31. Liu, Y., & Shi, J. (2020). Predicting the Potential Global Geographical Distribution of Two Icerya Species under Climate Change. Forests, 11(6), 684. https://doi.org/10.3390/f11060684.
32. Elith*, J., H. Graham*, C., P. Anderson, R., Dudík, M., Ferrier, S., Guisan, A., J. Hijmans, R., Huettmann, F., R. Leathwick, J., Lehmann, A., Li, J., G. Lohmann, L., A. Loiselle, B., Manion, G., Moritz, C., Nakamura, M., Nakazawa, Y., McC. M. Overton, J., Townsend Peterson, A., … E. Zimmermann, N. (2006). Novel methods improve prediction of species' distributions from occurrence data. Ecography, 29(2), 129–151. https://doi.org/10.1111/j.2006.0906-7590.04596.x.
33. Bozinovic, F., Ferri-Yáñez, F., Naya, H., Araújo, M. B., & Naya, D. E. (n.d.). Thermaltolerancesinrodents:Speciesthatevolvedincoldclimatesexhibitawiderthermoneutralzone.
34. McNutt, J. W., Groom, R., & Woodroffe, R. (2019). Ambient temperature provides an adaptive explanation for seasonal reproduction in a tropical mammal. Journal of Zoology, 309(3), 153–160. https://doi.org/10.1111/jzo.12712.
35. Ringani, G. V., Julius, R. S., Chimimba, C. T., Pirk, C. W. W., & Zengeya, T. A. (2022). Predicting the potential distribution of a previously undetected cryptic invasive synanthropic Asian house rat (Rattus tanezumi) in South Africa. Journal of Urban Ecology, 8(1), juac005. https://doi.org/10.1093/jue/juac005.
36. Abdel Rahman Ahmed, E. H., Ducroz, J.-F., Mitchell, A., Lamb, J., Contrafatto, G., Denys, C., Lecompte, E., & Taylor, P. J. (2008). Phylogeny and historical demography of economically important rodents of the genus Arvicanthis (Mammalia: Muridae) from the Nile Valley: of mice and men: PHYLOGENY OF NILE VALLEY ARVICANTHIS (RODENTIA). Biological Journal of the Linnean Society, 93(3), 641–655. https://doi.org/10.1111/j.1095-8312.2007.00895.x.
37. Desoky, A., Baghdadi, S., & Ahmed, H. (2014). POPULATION DENSITY AND SEASONAL DISTRIBUTION OF RODENT SPECIES AT SHEEP FARMING IN El-KAWTHER REGION, SOHAG GOVERNORATE, EGYPT. Journal of Plant Protection and Pathology, 5(10), 903–907. https://doi.org/10.21608/jppp.2014.88005.
38. Desoky, A. E.-A., Ahmed, A. M., & Salman, A. (2023). Survey and Population Density of Rodent Species in Abydos Area, Sohag Governorate, Egypt. 82–71 ,(2)3 ,□□□□□□□□□ □□□□□ □□□□□ □□□□. https://doi.org/10.21608/sjyr.2023.300340.

Figures

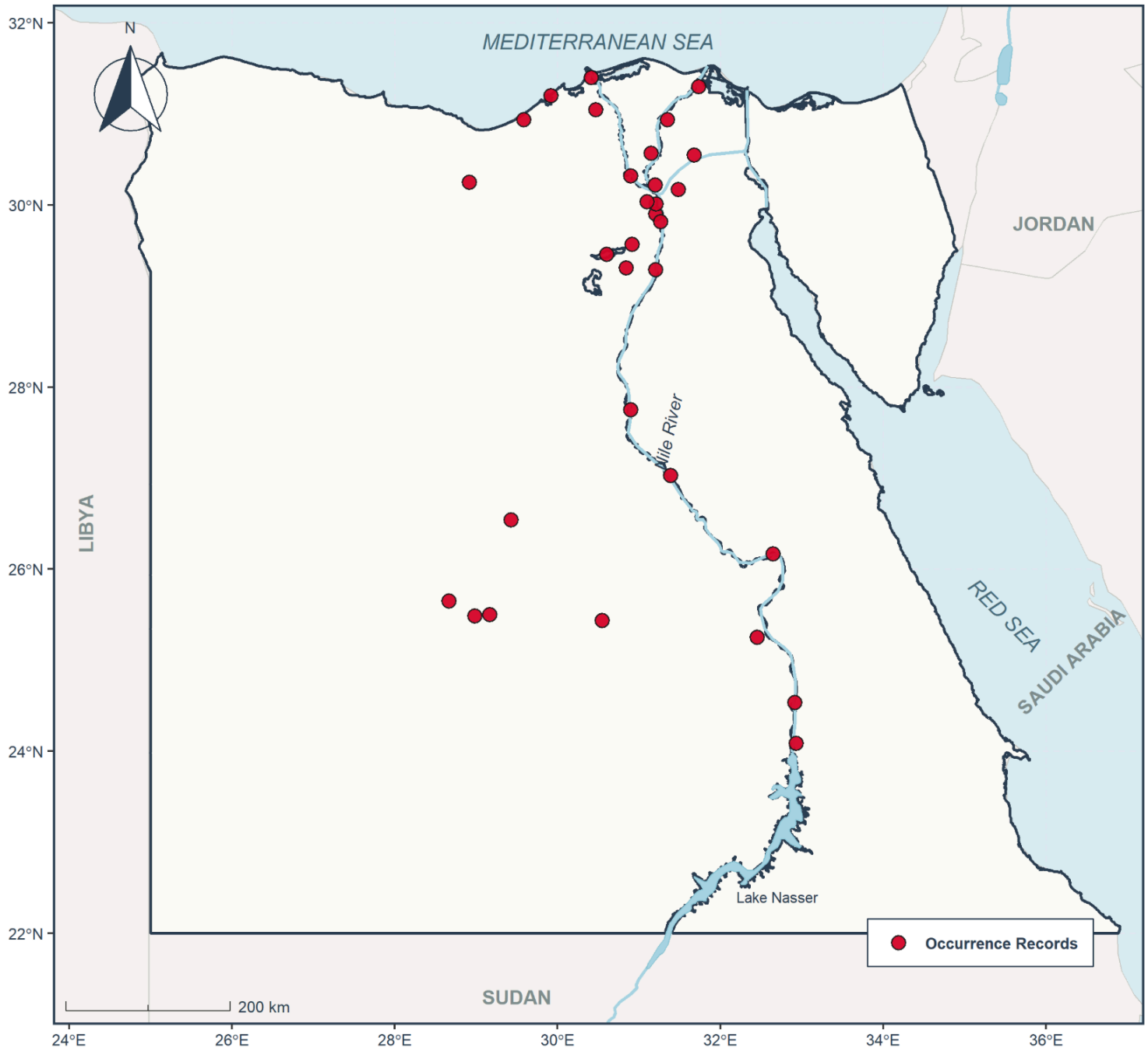

MEDITERRANEAN SEA
JORDAN
LIBYA
Nile River
RED SEA
SAUDI ARABIA
Lake Nasser
SUDAN
Occurrence Records
200 km
N
32°N
30°N
28°N
26°N
24°N
22°N
24°E
26°E
28°E
30°E
32°E
34°E
36°E

Figure 11

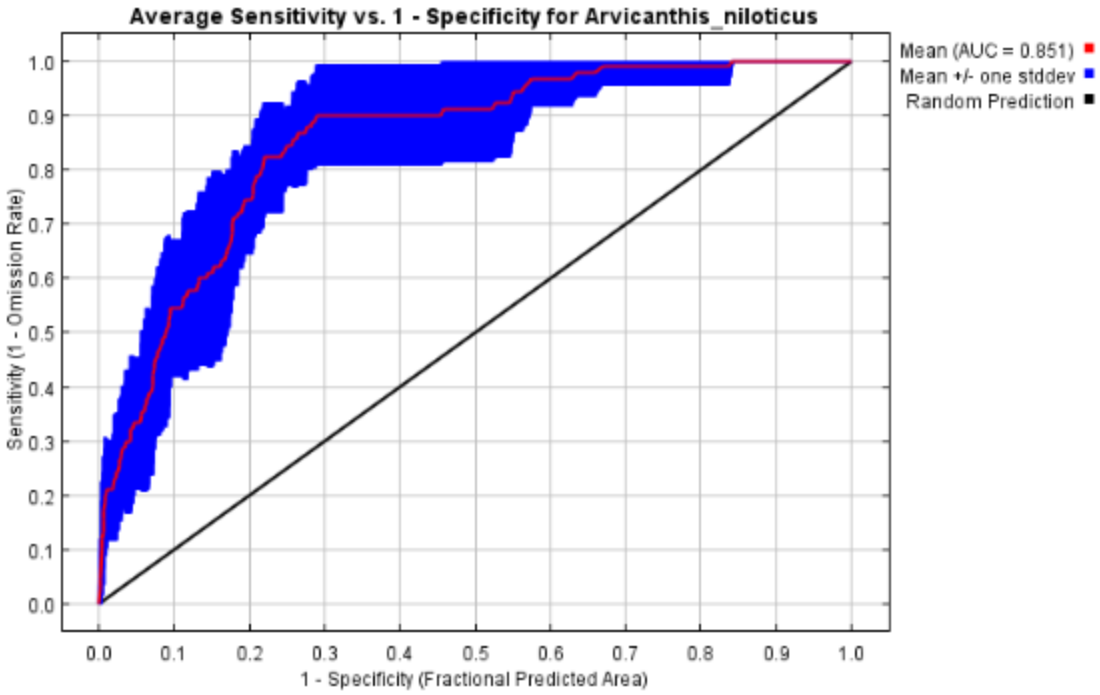

Average Sensitivity vs. 1 - Specificity for Arvicanthis_niloticus
Mean (AUC = 0.851)
Mean +/- one stddev
Random Prediction
Sensitivity (1 - Omission Rate)
1 - Specificity (Fractional Predicted Area)
0.0
0.1
0.2
0.3
0.4
0.5
0.6
0.7
0.8
0.9
1.0

Figure 12

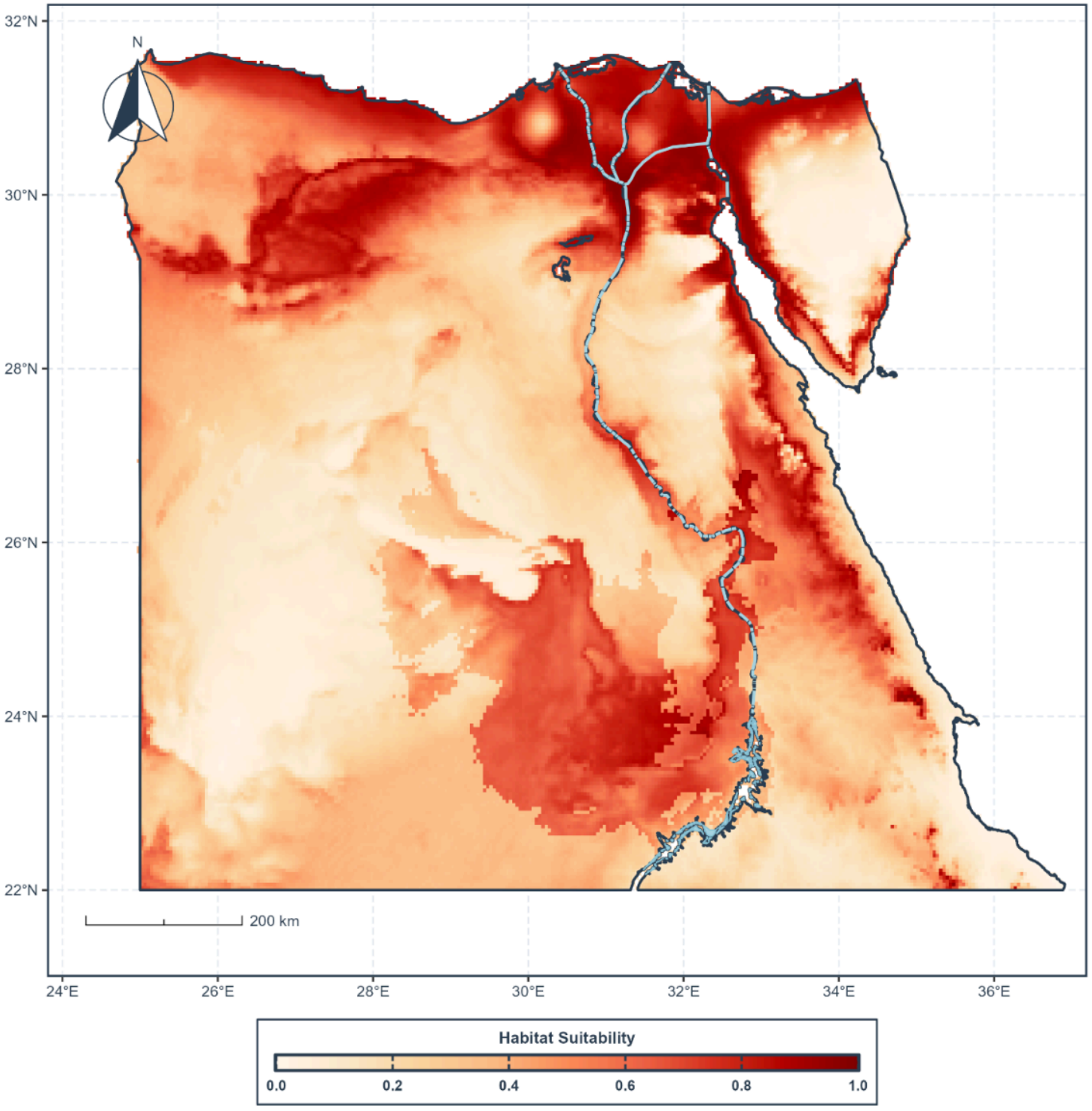

N
32°N
30°N
28°N
26°N
24°N
22°N
200 km
24°E
26°E
28°E
30°E
32°E
34°E
36°E
Habitat Suitability
0.0
0.2
0.4
0.6
0.8
1.0

Figure 13

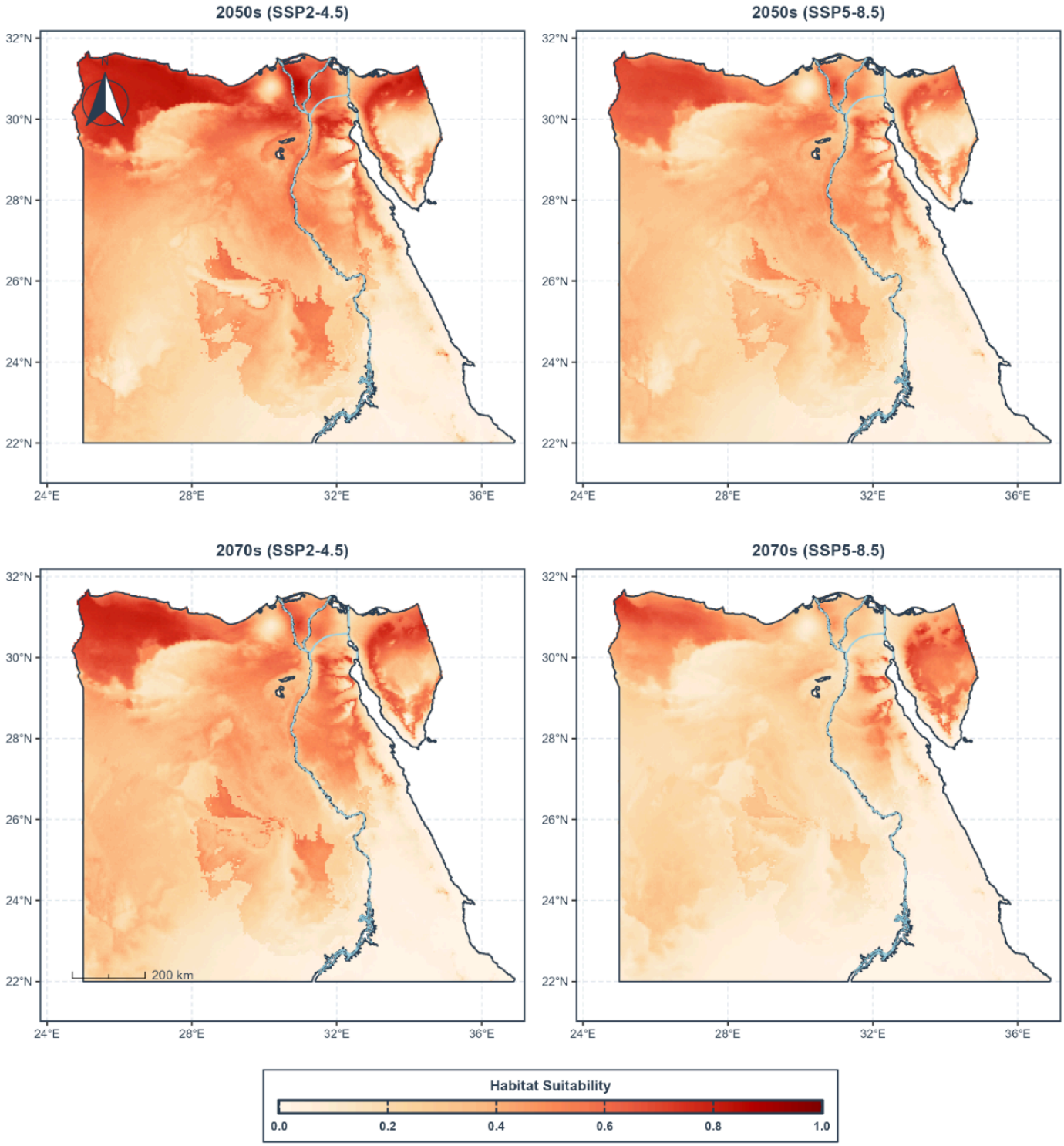

2050s (SSP2-4.5)
2050s (SSP5-8.5)
2070s (SSP2-4.5)
2070s (SSP5-8.5)
32°N
30°N
28°N
26°N
24°N
22°N
24°E
28°E
32°E
36°E
200 km
Habitat Suitability
0.0
0.2
0.4
0.6
0.8
1.0

Figure 14

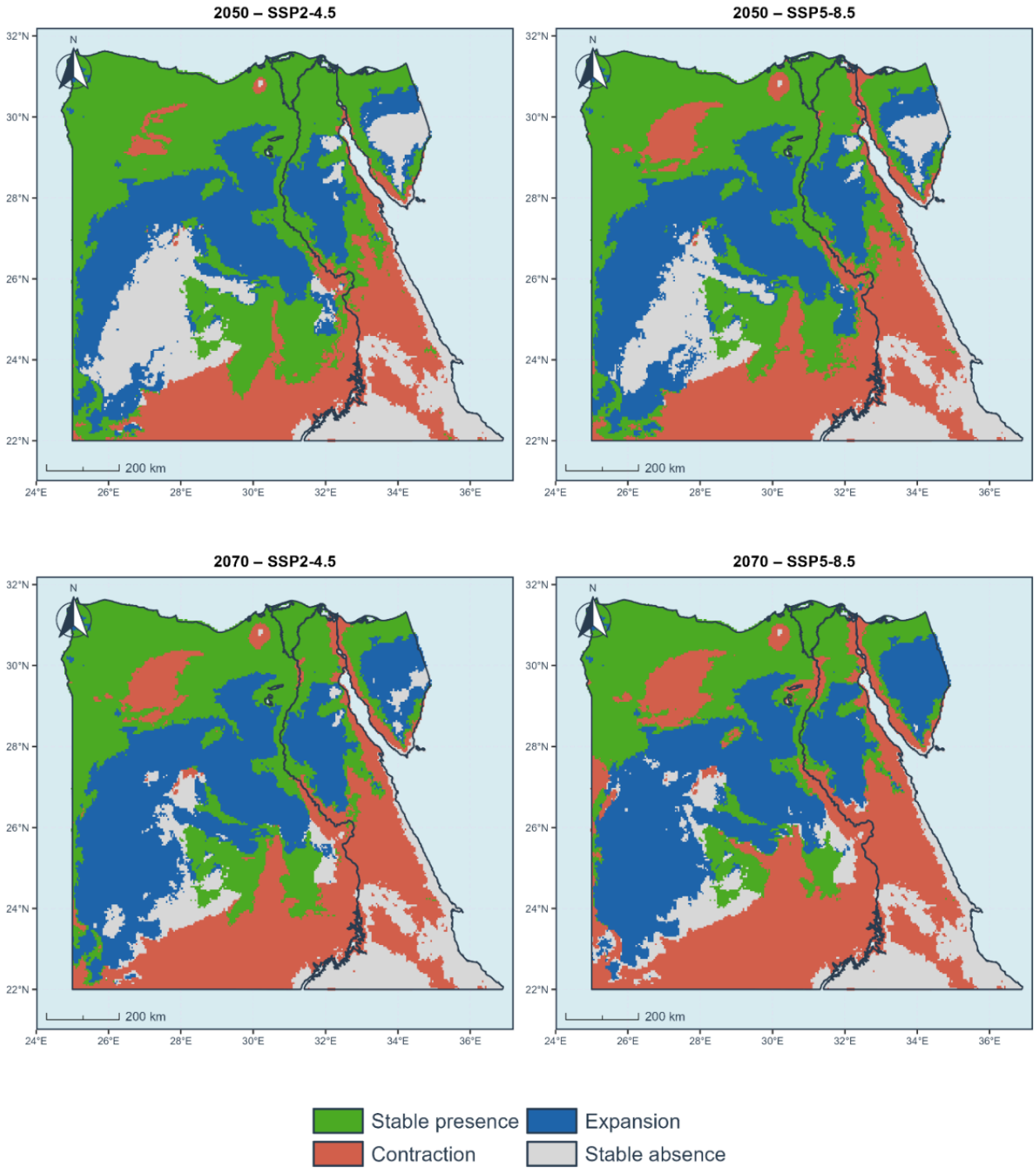


Figure 15

Supplementary Files

This is a list of supplementary files associated with this preprint. Click to download.

- FileS4.docx

- FileS2.docx
- FileS1.xlsx
- FileS5.xlsx
- FileS6.docx
- FileS8.docx
- FileS3.docx
- FileS7.docx